Case Study: Water and Ice

Timothy A. Isgro, Marcos Sotomayor, and Eduardo Cruz-Chu

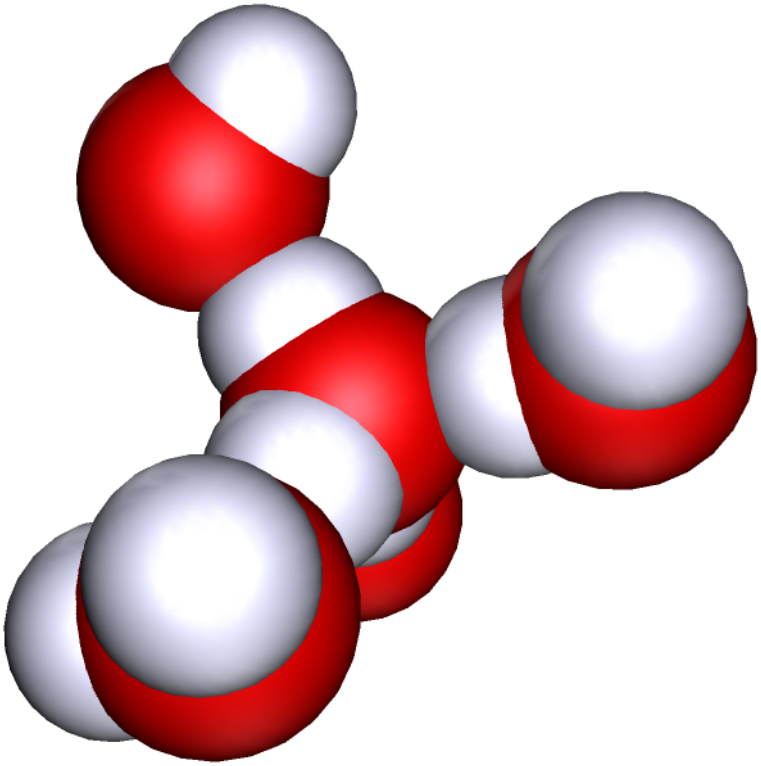

1 The Universal Solvent

Water is essential for sustaining life on Earth. Almost 75% of the Earth's surface is covered by it. It composes roughly 70% of the human body by mass [1]. It is the medium associated with nearly all microscopic life processes. Much of the reason that water can sustain life is due to its unique properties.

Among the most essential and extreme properties of water is its capability to absorb large amounts of heat. The heat capacity of water, which is the highest for compounds of its type in the liquid state, measures the amount of heat which needs to be added to water to change its temperature by a given amount. Water, thus, is able to effectively maintain its temperature even

when disturbed by great amounts of heat. This property serves to maintain ocean temperatures, as well as the atmospheric temperature around the oceans. For example, when the sun rises in the morning and a large amount of heat strikes the surface of the Earth, the vast majority of it is absorbed by the ocean. The ocean water, however, does not exhibit a drastic increase in temperature that could make it inhospitable to life. In constrast, when the sun sets in the evening and that heat is taken away, the oceans do not become too cold to harbor life. Water also has high latent heats of vaporization and melting, which measure the amount of heat needed to change a certain amount of liquid water to vapor and ice to liquid, respectively. These two properties also aid in the maintenance of ocean temperature.

An anomalous property of water, which is especially important for life in cold climates, is the occurrence of its maximum density at 4°C, just above the 0°C freezing point. Therefore, as water begins to drop in temperature when its surface is cooled, the water at the surface will reach this highest density. The surface water will then begin to sink, displacing the warmer water below itself. This results in the freezing of water from the surface downward. The effect takes place in ponds and lakes that are located in cold climates. Their surface freezes, and the water underneath remains liquid, protecting the organisms that live there.

Water vapor also plays a key role in determining the amount of energy from the sun which is retained on Earth. The spectrum of water vapor is such that the molecule is transparent to most radiation in the sunlight range, but it absorbs a considerable amount of infrared radiation at wavelengths typically emitted by the Earth upon release of the energy provided by the sun. Thus, water vapor is responsible for Earth's greenhouse effect and provides higher temperatures than would otherwise be expected on Earth.

Many other properties of water are no less surprising in their relationship to the development of life. Water maintains an identity as a "universal solvent", that is, it may serve to transport a multitude of chemical constituents throughout the bodies of living organisms. Water has the ability to ionize substances in solution which is important in establishing the proper electrostatic concentrations utilized by so many biological processes. Water also possesses an abnormally high surface tension, a property seen in the shape of water droplets and very important in living systems. The unique properties of water give it incredible versatility allowing it to foster and maintain a stable relationship with life on Earth. In this case study we will explore some of the properties of water mentioned above. The following files will be

used:

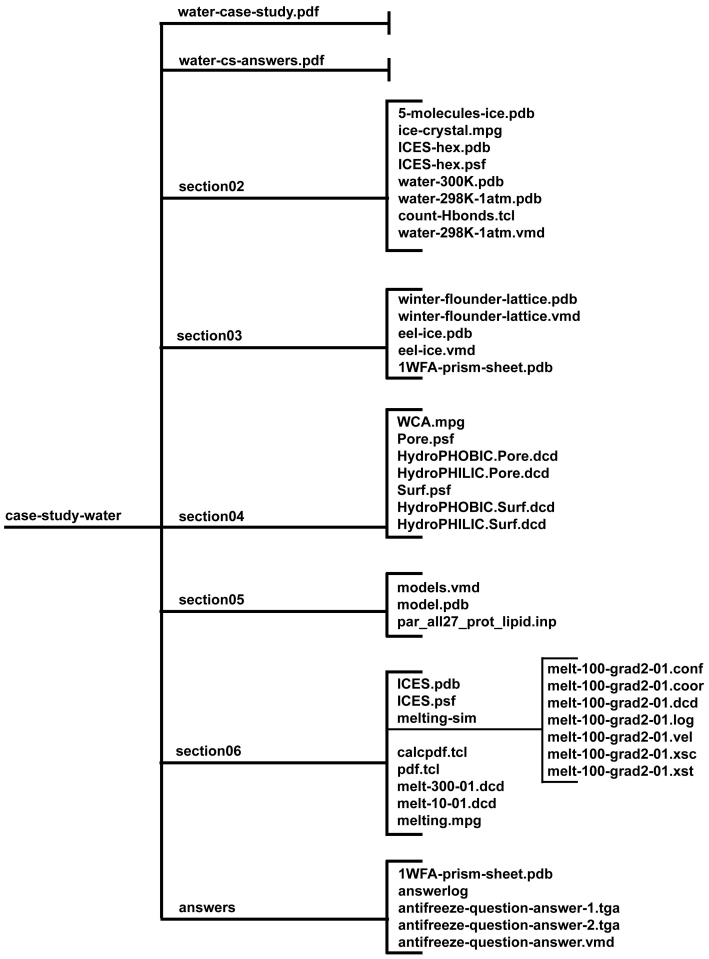

Figure 1: Files for the case study may be found on the Desktop of your laptop in the folder case-study-water/ or in BioCoRE as the file case-study-water.tar.gz. If it should become necessary for you to download the files from BioCoRE, do so and untar them with the command "tar -xzvf case-study-water.tar.gz". The folder case-study-water/ containing all files will be created in your working directory

2 The Liquid and Solid Phases of Water

Water exists above 100 °C as a gas, above 0 °C as liquid, and below 0 °C as ice. Here we describe the latter two phases that are biologically the most relevant.

2.1 Liquid Water

The fluid phase of any substance is usually the hardest to study at the microscopic level by theoretical means. Common approximations of non-interacting volumeless particles employed for ideal gases are not applicable for liquids, and neither are the elegant theories applied to periodic and symmetric systems found in solid phases. Experimental and theoretical descriptions of liquid phases are usually limited to macroscopic properties well described by continuous models. However, it is well known that hydrogen bonding between water molecules is important in establishing the structure of water, whether it be in solid or liquid form. The attraction which exists between molecules is indeed the reason for water's high boiling point, which is roughly 100°C higher than it would be if water was non-polar. If that were the case, all water on Earth would exist in gaseous form.

Although the microscopic structure of liquid water is unknown, the pair distribution function of liquid water (see Figure 15) obtained from experiments and simulations suggests that at short scales, water features an order that favors hydrogen bonding. However, molecules in liquid phase have enough kinetic energy to continuously form and break the bonds. Moreover, charged and polar solutes present in water under physiological conditions drastically influence the arrangement and bonding of water molecules surrounding them.

Experimental techniques to determine the structure of liquid water are lacking since each water molecule undergoes rapid rearrangement on the order of femtoseconds. The need for a better understanding of water at the microscopic level has forced the development of computational methods that describe the structure and dynamics of individual water molecules, and many studies have been carried out using these techniques. Many predict locally ordered hydrogen bonding whereby rings of molecules continually form and break. The rings may be made up of three to seven members, rather than the six-membered rings which exist in ice [1]. The rapidly changing nature of liquid ice structure, and of all liquids, for that matter, makes it very difficult

to study and characterize.

2.2 Ice

Hydrogen bonding is also responsible for the crystal structure of ice. Upon freezing at atmospheric pressure, water reduces the interaction energy between molecules by forming a regular network in which each molecule is hydrogen-bonded to four others. The oxygen atom bonds to two hydrogen atoms from other molecules and each hydrogen atom bonds to an oxygen atom from another molecule (Figure 2). With four hydrogen bonds per molecule, the ice crystal lattice conformation reduces the overall energy of the water molecules. The lattice also happens to be less dense than liquid water structure. In fact, the crystal structure of ice leaves enough room between molecules to fit entire other water molecules. The difference in density between liquid and crystal water is visible in Fig. 3. A movie of the crystal lattice of ice being formed is available in the file movies/ice-crystal.mpg.

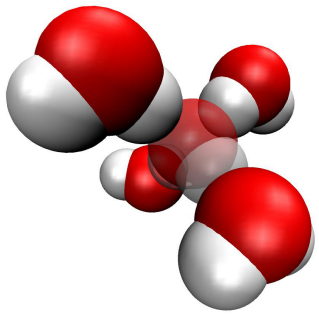

Figure 2: Five water molecules showing the arrangement of hydrogen bonding in crystalline ice. View the file 5-molecules-ice.pdb using VMD.

The structures of ice shown in Fig. 3 represent hexagonal ice, the type of ice that you are most familiar with, such as ice cubes in a glass or snow on the ground. However, it is not the only type of ice known. In fact, at least 14 phases of crystal ice are known to form depending on ambient pressure and temperature. Hexagonal ice, or ice 1h, is the form which exists at 1 atm and 0°C and is thus the type of frozen water found on Earth. As implied by its name, it is constructed of a hexagonal lattice of water molecules, a feature which is reflected by the 6-fold symmetry of snowflakes. The hexagonal lattice is commonly identified by four axes labeled a_1, a_2, a_3, and c (see Fig. 3). Note that all three "a-axes" are equivalent. The six lattice faces perpendicular to the a-axes are known as the "primary prism" planes and the two faces perpendicular to the c-axis are known as "basal planes". (The lattice may also be identified by three axes called a, b, and c, whereby a = a_1, b = a_2, and c = c.)

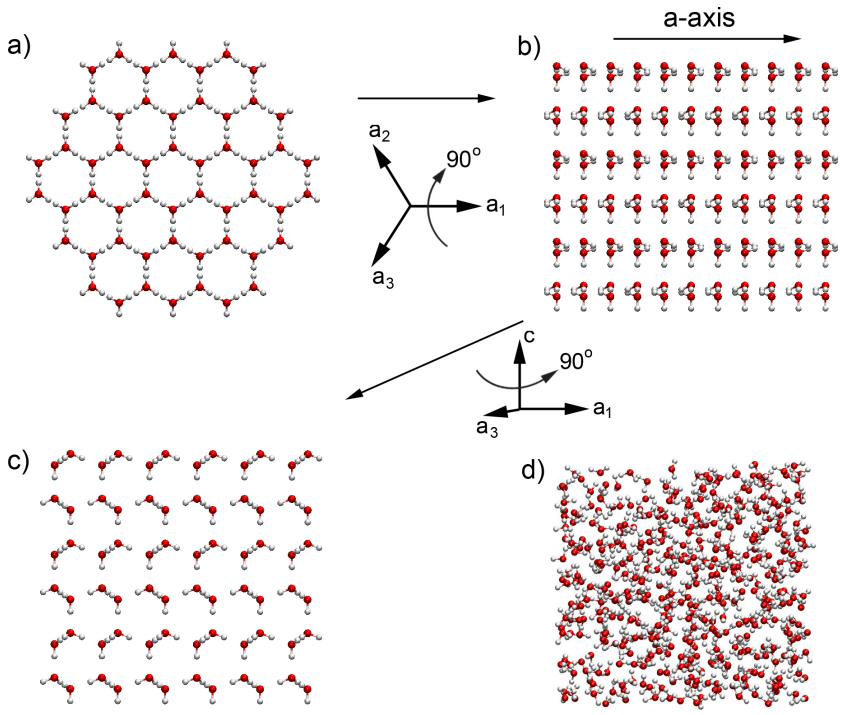

Figure 3: Views of the crystal structure of ice (a-c) and a view of liquid water (d). a) Along the c-axis of the lattice (showing the basal plane) with all 3 equivalent a-axes in the plane of the page and the c-axis coming out of the page, b) With an a-axis running left to right (showing the primary prism plane), c) Along an a-axis, d) Liquid water at 300 K. The difference in the density between ice and liquid water is apparent. The density of liquid water at 4°C is 1.00 g/cm^3, while that of ice at 0°C is 0.917 g/cm^3 [2]. View the files section02/ICES-hex.pdb (a-c) and section02/water-300K.pdb (d) using VMD.

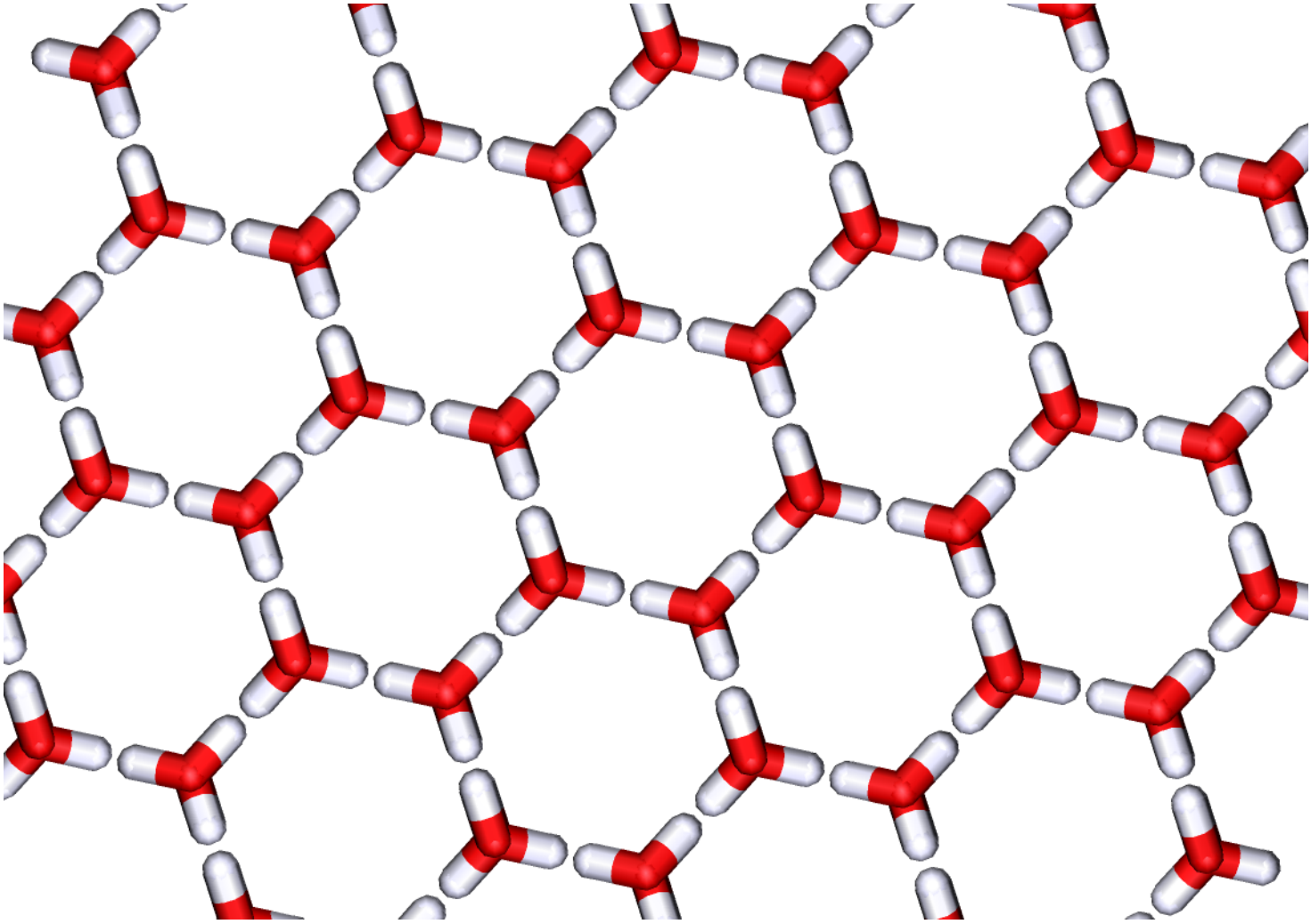

Basal Plane	Primary Prism Plane	Along an a-axis

Exercise 1: Hydrogen bonding. In ice 1h, each molecule is hydrogen bonded to four others. However, in liquid water, that number varies from molecule to molecule.
(1) Do you think the number of hydrogen bonds in liquid water should be more or less than four? Why? Load the file water-298K-1atm.pdb, a snapshot of equilibrated water at 298 K and 1 atm, into VMD. Count the average number of hydrogen bonds for each molecule by running the script count-Hbonds.tcl using the "source" command in the TkConsole. Make sure before hand that you are in the right directory; you may have to first change the directory with the command "cd case-study-water/section02" in the TkConsole. Note that we are using a less stringent criteria to select hydrogen bonds and do not take into account the bond angle.
(2) Load the VMD saved state water-298K-1atm.vmd. Use VMD to count the number of hydrogen bonds that the three water molecules shown in color make with other molecules: (a) green, (b) orange, (c) yellow. Use 2.6 Angstroms as a cutoff for hydrogen bonding. Give the number of hydrogen bonds for each of the three molecules along with the resid's of the molecules to which it is hydrogen bonded. Since bond angles are not being considered for the present exercise, do not use the Hbonds drawing method of VMD, but rather measure distances directly between each molecule and its neighbors using VMD.

3 Antifreeze Proteins

The ability of atomic and molecular substances to change the behavior of water by lowering its freezing point or elevating its boiling point is evident to most people, especially on cold winter days when salt is scattered on streets to prevent ice from forming. Nature, too, has a means of causing the "freezing point depression" of water. It uses proteins and the crystalline regularity of ice to carry out the task.

Thermal hysteresis proteins, or antifreeze proteins (APs) as they are sometimes referred to, enable nature the same type of control over the freezing of water as that afforded to street salters. However, the manner in which water interacts with the AP differs from salt. Whereas freezing point depression via adding sodium chloride to water is a colligative property (the effect is proportional to the number of particles added), the freezing point depression which antifreeze proteins induce is noncolligative. The reason is that APs act by binding to ice surfaces already formed and inhibiting the further formation of ice, rather than by altering the properties of cold liquid water.

AP Type	Typical Size (kDa)	Secondary Structure	Amino Acid Features
Type I	3.3-4.5	α-helical	$ThrX_2AsxX_7$
Type II	6-14	globular	disulfide bridges
Type III	6-14	globular	none
Type IV	12	4 amphipathic α-helices	Glx-rich

Table 1: Properties of the four types of antifreeze proteins. It is interesting to note that the types exhibit notable variety in structure and composition, yet perform essentially the same task.

To understand specifically how APs work, one must relate their structure to the crystal structure of ice. In accordance with usual growth of crystalline solids, normal ice growth takes place along the axis with the highest atomic density, the a-axes in this case (see Fig. 3b). APs take advantage of this fact by binding to faces, or planes, of ice which intersect the a-axes, restricting ice growth.

APs are found in many cold-surviving animals, such as fish and insects. Fish APs have been the most widely studied both experimentally and computationally. All APs are categorized into one of four types (Table 1). What makes them perhaps most interesting is that while all APs perform the same basic task, each type is quite different in structure. We will use VMD to investigate a type I AP, and then look at a possible ice recognition motif for a type III AP.

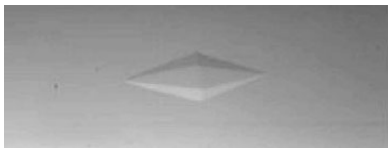

Figure 4: Ice crystal formation in a glass capillary in the presence of winter flounder type I antifreeze protein. The shape reflects the binding of winter flounder AP to the pyramidal $\{20\bar{2}1\}$ plane of ice. Picture from [3].

Type I APs are typically small proteins, roughly 3.3-4.5 kDa in size and composed of α-helical secondary structure. Most type I APs consist of the amino acid repeat $ThrX_2AsxX_7$ which binds to ice. Based on ice etching experiments, it has been determined that HLPC6, a winter flounder type I AP, typically binds to the $\{20\bar{2}1\}$ plane (equivalently $\{201\}$ in a, b, c-axis notation) of ice 1h along the $\langle 01\bar{1}2\rangle$ direction in which the ice oxygen atoms have a repeat distance of approximately

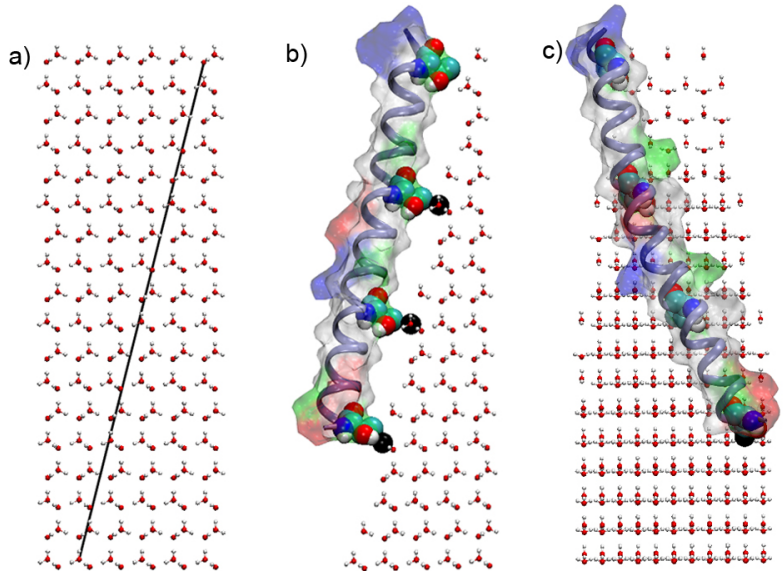

Figure 5: Winter flounder antifreeze protein HPLC6 bound to the $\{20\bar{2}1\}$ plane of ice. a) A $\{20\bar{2}1\}$ plane cut into the ice crystal. The a-axis points out of the page as in Figure 3c. b) HPLC6 bound to the surface. Note the regular spacing of Thr residues shown in vdW representation, which match the ice lattice spacing. The oxygen atoms to which Thr residues bind are shown as black spheres. c) A "front" view of the binding. The a-axis runs left to right parallel to the page. View the file section03/winter-flounder-lattice.pdb and the saved state section03/winter-flounder-lattice.vmd using VMD.

16.7 Å [4]. Figure 5 shows how macroscopic ice formation is affected by the presence of winter flounder AP. The effect of flounder AP on the formation of ice crystals reflects the atomic properties of the proteins binding to the ice surface.

Indeed, the protein's sequence and structure seems to fit the $\{20\bar{2}1\}$ motif quite nicely. HPLC6 is a single α-helix with threonine residues lining one side of the helix and having a distance of approximately 16.7 Å between them. It is thought that the protein uses this perfect structural complementarity to ice to bind to the surface of the crystal and inhibit its growth [5]. Figure 6 shows the protein bound to a $\{20\bar{2}1\}$ plane of the ice lattice. Note the regularity of the threonine residues which is a perfect complement to the lattice periodicity. The transparent surface of the protein, which is colored by residue type, also displays an interesting feature of the protein. One side of the protein is lined very regularly with hydrophilic residues (white

is hydrophobic), as mentioned, which may lead one to believe that binding occurs via these residues. However, mutation experiments and computer simulations have led to a second hypothesis which states that the hydrophobic residues along the helical surface are the ones that are actually important in the protein recognizing the ice surface [3, 6]. Only after such recognition may the hydrophilic residues bind to the crystal. The drastic contradiction between the two models poses a very fundamental question which remains unanswered: "Is ice more hydrophobic than water?". Computational and experimental studies being conducted today may provide the answer.

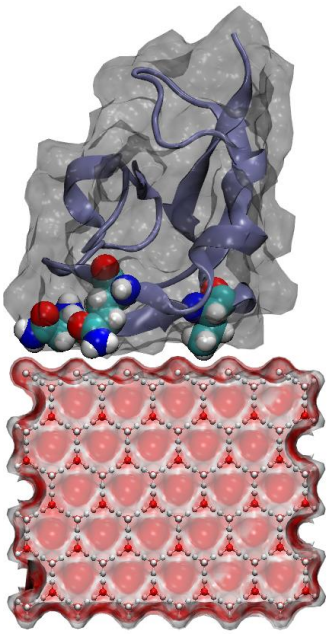

Figure 6: Ocean eel pout type III antifreeze protein showing surface complemetarity to the primary prism face of ice. Residues N14, T18, and Q44 are shown in vdW representation. View the file section03/eel-ice.pdb and the saved state section03/eel-ice.vmd using VMD.

Type III APs differ from their type I counterparts in several ways. They are typically larger, 6-14 kDa in size, globular in structure, do not contain a dominant amino acid residue like type I APs (Ala), and lack any apparent repeat sequence of amino acids. As a result, it is very difficult to predict how a given type III AP will bind to ice. It is known from ice etching experiments, however, that the most prominent face to which type III APs bind is the primary prism plane {100} of ice [5], which is shown in Fig. 3b. The antifreeze protein from ocean eel pout has been classified as a type III AP, and conserved hydrophilic residues N14, T18, and Q44 have been identified as essential to antifreeze activity. These residues make up a face of the protein which is unusually flat. As in the case of type I APs, surface complementarity with ice is believed to be important, too. By examining the crystal structure of ocean eel pout AP, in relation to the primary prism crystal plane of ice, we are able to see the surface complementarity established by the three residues (see Fig. 7). It may also be interesting to note that the fourth residue (not highlighted) which adds to the surface complementarity is A16. A

simple look at the molecule's surface when paired with ice may be enough to identify the ice binding mechanism. Indeed, energy minimization calculations of ocean eel pout have established that low energy configurations of the protein-ice surface exist when "lattice matching" is established, just as in type I APs [5].

While seeing a possible ice binding motif is interesting in its own right, researchers are also interested in exactly how the protein recognizes and attaches itself to ice, that is, the binding mechanism. In fact, ocean eel pout AP induces steps to form in the ice surface, leading to the hypothesis that residue N14 initiates binding of the protein to the crevice between basal $\{001\}$ and primary prism planes $\{100\}$ of ice [7]. Molecular dynamics is an ideal method to test such a hypothesis, but in order to do so one must know how to represent, or model, the water which our protein will be solvated in and binding to. Before giving a description of these kind of microscopic models, we will explore in the next section some properties of liquid water.

Exercise 2: Type I AP binding. The originally proposed [8] binding mechanism for type I AP HPLC6 had the protein binding to the primary prism plane of ice. This may have been the most obvious choice, as ice grows perpendicular to this plane, but ice etching experiments [4] proved it to be wrong. Try to replicate the thought process of early AP scientists by figuring out the best possible docking of HPLC6 on the primary prism face of ice. The file 1WFA-prism-sheet.pdb contains a sheet of primary prism face ice along with HPLC6. Use VMD translate and rotate commands in the TkConsole, such as "$HLPC_selection moveby {1 2 5}" and "$HLPC_selection move [trans axis x 40 deg]", to move the protein into a hypothetical docked position on the ice, which takes advantage of the protein's threonine repeat distance. Note that the fit will not be as good as for $\{20\bar{2}1\}$ binding. Emphasize the ice oxygen atoms (as vdW spheres, for instance) with which the protein make contact. Create two VMD snapsots from different angles.

4 The Wettability of Water

The importance of water in sustaining life processes is very apparent. On the nanoscopic level, living organisms have evolved proteins which are precisely tuned to take advantage of a water environment. For cold-dwelling organisms, the interaction between water and its antifreeze proteins prevents freezing in extreme conditions. On the macroscopic level, some life forms

have evolved features to take advantage of another interesting property of water: its high surface tension.

The "wetting behavior" of a surface, its ability to interact with a liquid, can be characterized by the surface tension of the liquid as well as the features of the solid surface. Qualitatively, good wetting behavior is observed if a liquid spreads widely over a certain surface, and non-wetting behavior is observed if the liquid tends to avoid the surface, forming small droplets. We will begin with an investigation of the physics behind surface wetting and later see how one insect has evolved features to benefit from water's surface tension in an exquisite and surprising way.

Figure 7: A picture of a water strider standing on the surface of water. Note the extensive surface coverage of the back legs. Picture from http://www-math.mit.edu/%7Edhu/Striderweb/adultside.jpg

4.1 The physics of surface tension

In order to understand the wetting behavior of liquids, we need to understand the microscopic molecular organization of a homogeneous liquid. In a liquid state, molecules are free to move in relation to one another but at the same time are in close contact. Due to their close proximity, intermolecular forces between molecules, which are typically irrelevant in gases, play a major role in establishing the properties of the liquid.

A closer view into a liquid structure reveals that not all molecules within the liquid are under the same influence. In general, we can separate the molecules into two groups: those moving freely in the bulk while others are transiently captured at the surface. This is because each molecule at the surface has interacting neighbors only at one side, and the resulting force is in the direction of the bulk. The energy of a surface molecule is therefore higher than that of a bulk molecule, and energy must be expended to move a molecule from the interior to the surface. This energy distribution on the surface is responsible for the phenomenon known as surface tension.

Surface tension is measured in units of force per length (typically dynes/cm), and it quantifies the amount of force required to break a liquid film of given length. An equally meaningful quantity is the "surface free energy", measured in units of energy per area (typically ergs/cm^2). Even though both names qualitatively describe the same phenomenon, the term "surface tension" is older and consequently used more [9] . Water has a surface tension of 72.8 dynes/cm at 20°C and 1 atm.

To minimize the free energy of the system, liquids tend to form shapes that reduce their surface. As a result, drops and bubbles are spherical, since the sphere has the lowest surface/volume ratio. Even though gravity breaks that ideal geometry, causing liquids to fit into the container shape, the final form always tends to minimize the exposed surface [10] .

By 1800, Laplace realized that the spherical shape also leads to a pressure difference between the two sides of the surface and stated a simple equation that correlates pressure difference, surface tension, and the radius of the sphere:

$$P_{in} = P_{ex} + 2\frac{T}{r} \tag{1}$$

where P_{in} is the internal pressure, P_{ex} is the external pressure, T is the surface tension, and r is the radius of the sphere [9]. The equation states that the pressure inside of a curved surface is always higher than the pressure outside. The pressure difference is cancelled when the curvature ratio tends to be infinite, i.e., the surface is flat.

4.2 Wetting a surface

When a liquid is in contact with an inert solid phase, the liquid "wets" the surface. Liquid molecules at the solid-liquid interface are now in a differ-

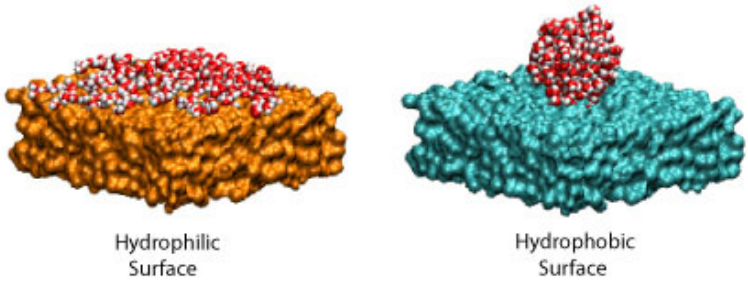

Figure 8: The wetting behavior of a water droplet depends on the surface characteristics. Over a hydrophilic surface, the water droplet spreads. Over a hydrophobic surface, it tries to avoid contact and forms a bubble. This figure was created from the trajectories associated with Fig. 11.

ent environment than the ones that are either in the bulk or at the exposed surface. Those molecules feel two kinds of forces: cohesive forces acting between like molecules and adhesive forces acting between different molecules. The balance between cohesive and adhesive forces determines the wetting properties of the surface (Fig. 9). When the cohesive forces of water can be counterbalanced by the adhesive forces of the substrate, a liquid droplet tends to spreads over the surface. When the cohesive forces of water are stronger than the adhesive forces of the substrate, the droplet tries to avoid the surface, keeping its spherical shape and reducing the surface tension.

Think about a tiny water droplet resting on an inert solid surface, such as your desk. Within the droplet, water molecules are held together by cohesive forces. At the interface between the water droplet and the desk, adhesive forces emerge. However, cohesive forces are stronger and surface tension will still hold the droplet in a roughly spherical shape (unless your desk is quite exotic).

4.3 Water Contact Angle

We now introduce a method to evaluate the balance between the solid surface-liquid water interactions by using one of the most sensitive, beautiful, and

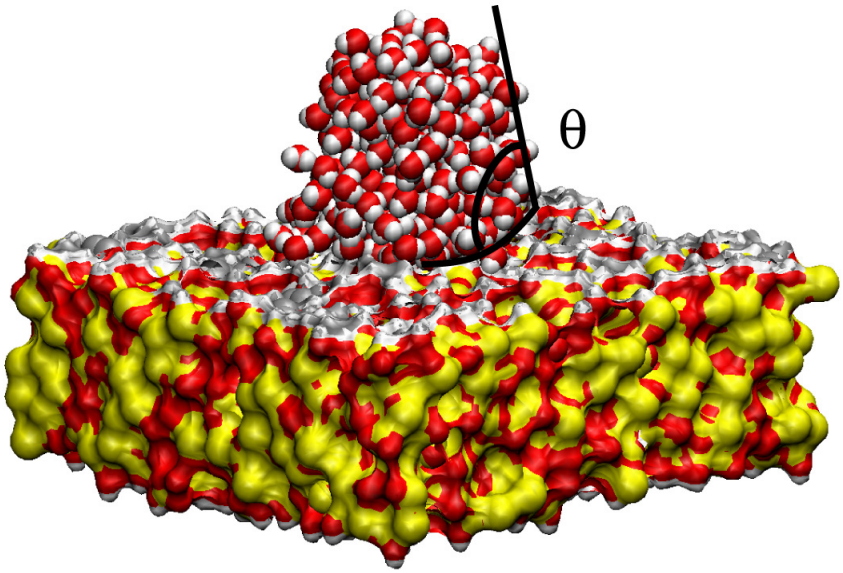

Figure 9: Water droplet resting on an inert surface. The contact angle is defined by the angle between the solid surface and the tangent to the surface liquid at the solid-liquid interface. View the movie section04/WCA.mpg.

cheapest instruments in the world: a small water drop.

Consider a water drop on a smooth and clean surface. The droplet will either spread completely over the surface, partially, or not at all [11]. This behavior may be quantified by the water contact angle (WCA), the angle between the tangent to the surface of the liquid and the tangent to the surface of the solid at the solid-liquid interface (Fig. 10). If the contact angle between a liquid and a solid is close to zero, the surface is considered "wet". If the angle is close to or greater than 90°, the liquid does not wet the surface. Wetting is analogous to hydrophobicity in that it reflects the degree of interaction of certain molecules with water. For a WCA greater than 150°, the surface is considered "superhydrophobic".

Macroscopically, the water contact angle of a droplet in equilibrium with

the surface is described by Youngs equation:

$$\cos\theta = \frac{\sigma_{SV} - \sigma_{SL}}{\sigma_{LV}} \tag{2}$$

where θ is the contact angle, and the σ symbols denote the surface tensions of each interface: solid-vapor, solid-liquid, liquid-vapor. Young's equation was stated in 1805 and describes the equilibrium relationship between the interfaces [12].

Microscopically, the water contact angle depends on the solid's surface topology as well as the specific solid-water interactions. We will explore one of the most popular surfaces, silicates, also known as glasses. Exposed functional groups establish the accessible regions that interact with other molecules and thus determine the silica wetting properties. At the silica surface, we have two functional groups: siloxanes (-O-Si-O-) and silanols (-Si-OH). The silanol group, with its hydroxyl group, is the dominant factor for hydrophilicity, attracting water to the surface. As more silanols are exposed, the surface becomes more hydrophilic. Conversely, a complete dehydroxylated silica surface, without silanols, is less hydrophilic, and would exhibit a WCA of around 44° [13].

Molecular dynamics allows one to explore the behavior of a silica surface in contact with water (Fig. 11). One can use the experimental values for the silica WCA to calibrate silica force fields, the set of equations and parameters that define the molecular interactions. Once the force field is calibrated, one can explore many scientific questions involving water-silica interactions, like water permeation (Fig. 12).

4.4 Walking on water

The mechanical motion of the water strider is a charming example of how nature exploits the surface tension of water to an advantage. Water striders are small insects that live on the surface of ponds and quiet rivers. They are typically a few centimeters in length, although some varieties like *Gigantometra gigas* have legs up to 20 cm long. As their name suggests, these insects can walk on water! The surface of water is quite an unsuitable place for many insects, so water striders take advantage of this to populate, feed, and breed themselves.

Three pairs of long hydrophobic legs are the secret of the strider's mobility. Precisely engineered to support their light weight, these legs have

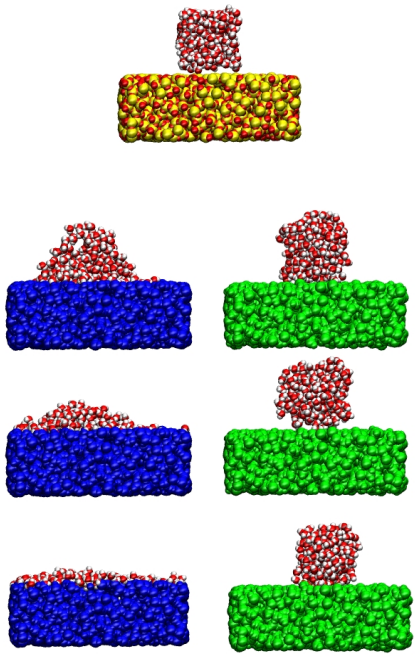

Figure 10: Force field (FF) parameters determine the wetting behavior in molecular dynamics simulations. For the same system two different silica force fields were evaluated. The top figure corresponds to the starting set-up: 699 water molecules in a cube of 18 Å and a dehydroxylated silica slab of $59 \times 59 \times 20$ Å. The silica for the two different force fields are pictured blue [14] and green [15]. Snapshots correspond to different time during the simulations: 20, 50 and 100 ps. View the simulations by loading the file section04/Pore.psf and either section04/HydroPHOBIC.Pore.dcd or section04/HydroPHILIC.Pore.dcd into it using VMD.

thousands of little hairs which are covered in wax. A careful combination of topology and structural features in the legs allow these insects to stand and "walk" without piercing the water. Recent studies [16] proposed that the particular arrangement of hair at the legs surface is the key factor for understanding their exceptional hydrophobicity. Accurate measurements of the WCA reveals a "superhydrophobic surface", with an angle of 167.6°!

Standing on the water surface is a basic mechanics problem. In order to remain afloat, the weight of the strider must be supported by a force in the opposite direction. That compensating force can come from two sources: the buoyancy force like in a swimming boat (via Archimedes principle) and/or

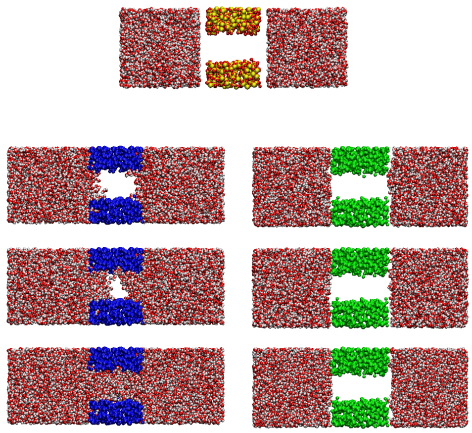

Figure 11: Permeation of water through a silica nanopore for two different force fields (c.f. Fig. 11) [14, 15]. The top snapshot shows the initial set-up of the system: a silica pore of 20 Å diameter and 37 Å height and two water boxes, each box with 6062 water molecules. Remaining snapshots correspond to different times during the simulations, namely, at 50, 100 and 190 ps. View the simulations by loading the file section04/Surf.psf and either section04/HydroPHOBIC.Surf.dcd or section04/HydroPHILIC.Surf.dcd into it using VMD.

surface tension. In the case of the water strider, the weight is essentially counterbalanced by surface tension, and buoyancy is irrelevant, since the volume of water displaced by the strider is very small. As the strider stands on the surface, their hydrophobic legs push the water downwards, generating a concave curvature surface around each leg. Thus, the vertical component of the surface tension force is in the upward direction and is proportional to the surface area of the water-leg interface.

Water striders propel themselves using their middle legs, achieving speeds of 1.5 m/s [17], while the back legs are used to steer and brake. The middle legs can apply force five times larger than the strider's weight. Conveniently, a single superhydrophobic leg can stand 15 times the strider's weight before piercing the surface [16].

Superhydrophobic surfaces are not exclusive properties of water striders. Lotus and rice leaves, to keep them from getting soaked, also have superhydrophobic surfaces [18], formed by capturing air to avoid contact with water. Nature has tuned the properties of these surfaces with a meticulous combination of non-wetting materials and nanostructures to the benefit of the

organism.

5 Modeling Water at the Molecular Level

We have learned already about the relevance of water in many aspects of our everyday life. In particular, its role in biological processes is fundamental, but sometimes not completely understood at the atomic level. How can one explore the microscopic behavior of water and thereby predict or explain its role in biological systems? Experiments, of course, allow the measurement of many properties of water like density, diffusion coefficient, heat capacity, and melting and boiling temperatures. However, theoretical and computational modeling, especially taking into account current advances in computer simulations, provides insight into systems in which water plays a fundamental role at the microscopic level.

The computer is becoming a microscope that can see scales experiments cannot reach, but, of course, the accuracy of the computational description depends on the underlying theoretical model of water. A model needs to reproduce the known behavior of water and, at the same time, predict unknown properties. While continuum models effectively reproduce macroscopic properties of water, the discrete nature of water molecules and their interaction and influence on the dynamics of molecular structures needs to be taken into account every time a biological system, i.e., a protein, derives function from interaction with individual water molecules. This is indeed the case very often.

The water molecule seems, at first glance, simple and easy to model. It has two hydrogen atoms and one oxygen atom with overall charges of $+1$ e for each hydrogen and -2 e for the oxygen atom. However, a great deal of information needs to be accounted for in a model. Where are these charges located? Are these charges distributed in a spherical, uniform, and symmetrical arrangement? How far are the hydrogens from the oxygen? What is the angle formed by the hydrogens and the oxygen? Is this a flexible or rigid molecule? How does it interact with the surrounding molecules? All these questions and many others need to be addressed for a faithful description of water and its role in living cells.

5.1 Explicit Water Models

With some simplifying assumptions, a basic theoretical water model can be constructed [19]. Imagine that the charges can be considered as point charges located at the center of each atom. Furthermore, assume the distance between atoms H and O and the HOH angle are fixed. Actually, if we use the location of the nuclei to place the charges, the dipole moment will be excessively high. By shifting the position of the negative charge from the oxygen atom towards the hydrogen atoms along the HOH angle bisector, we can decrease the dipole moment and improve the model (see Fig. 13a). In addition, we need to take into account the fact that molecules actually do not overlap. We can incorporate this property into our model by defining a Lennard-Jones like spherical repulsive potential centered in the molecule. If two molecules get too close to each other, forces originated from this repulsive potential will push them apart. The rigid theoretical model we just have constructed was actually proposed in 1933 by Bernal and Fowler, and can be considered the forerunner of subsequent three-point-charge models such as single point charge (SPC) and transferable intermolecular potentials (TIPS), both widely used in simulations of biomolecular systems [20]. In 1949, Rowlinson proposed another theoretical model of water using a very similar approach to that used by Bernal and Fowler, but the negative charge was split above and below the molecular plane at the oxygen center (see Fig. 13b) in order to reproduce the quadrupole moment of the water molecule [19]. Accordingly, the Rowlinson model can be considered as the forerunner of subsequent multipoint charge models used in computer simulations such as TIP4P, TIP5P, and others [19].

Once the basic characteristics of the theoretical model are set (number of charges, geometrical arrangement, type of interaction potentials, etc.), the parameterization process that follows can become extremely complicated. Small changes in the parameters can have relevant implications for the macroscopic properties of water, such as density, diffusion coefficient, and specific heat. Moreover, current theoretical models used in simulations of water include separate spherical dispersion and repulsion terms for the hydrogens and oxygen, as well as flexible harmonic bonds between the water molecule atoms. These are called intra-molecular interactions. In some cases, even the non-additive nature of water molecule interactions is included as molecular polarizability. All these new properties present a challenge for both the force field parameterization and the simulation itself, which needs to deal with

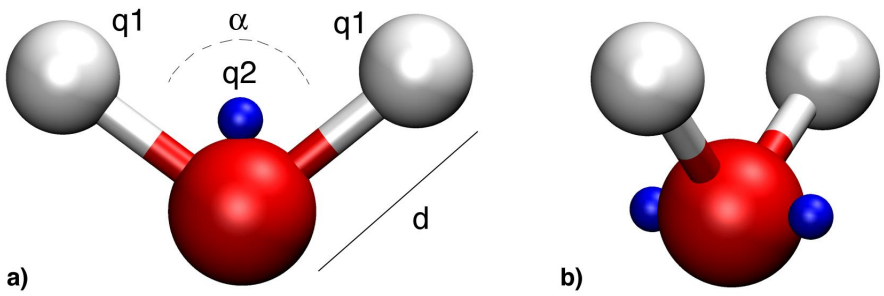

Figure 12: Water molecule models. **a**) Three site model of a water molecule in which the hydrogen atoms (white) and the oxygen atom (red) are linked through rigid or flexible bonds. The positive charges are located at the nuclei of the hydrogen atoms. The negative charged is located along the HOH angle bisector (blue sphere). Current models used in computer simulations, SPC and TIP3P, are based on this kind of arrangement. **b**) Four site model of a water molecule. Hydrogen atoms (white) and the oxygen atom (red) are linked through rigid or flexible bonds. In this case, the negative charge is split in two (blue spheres) and located above and below the oxygen nuclei. Use the available VMD state section05/models.vmd to further explore the water molecules presented in this figure.

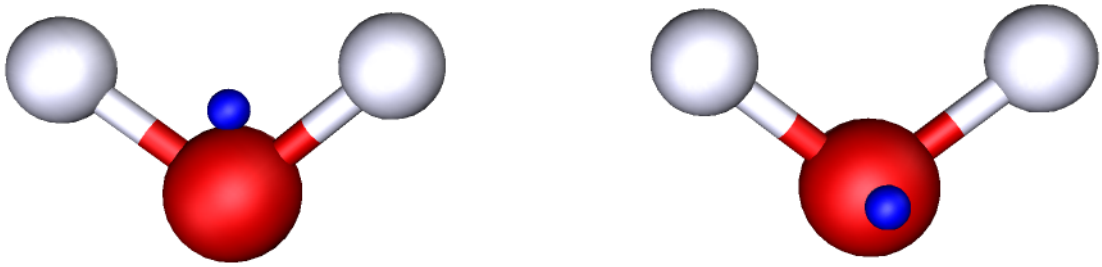

Two models **Three-point model** **Four-point model**

more complicated and costly computations. Many of these models are still under development and certainly fail to reproduce all properties of water as determined by experiments [20].

Two of the most popular models of water used in simulations of biomolecular systems are SPC and TIP3P. Both use three point charges but their respective parameters are slightly different. For instance, the equilibrium HOH angle is 109.47° in the SPC model, and 104.52° in the TIP3P model. The SPC parameters have been chosen to reproduce energy and pressure of liquid water at ambient conditions, as well as the second peak in the radial distribution function of oxygen atoms (see Section 6.2). The TIP3P parameters have been chosen to yield reasonable structural and energetic results for both gas-phase dimers and pure liquids. The values of the dipole moment, dielectric constant, and self diffusion coefficients for some popular models used in computer simulations are provided in Table 5.1.

Model	Dipole moment, D	Dielectric constant	Self Diffusion 10^{-5} cm^2/s
SPC	2.27	65.0	3.85
TIP3P	2.35	82.0	5.19
TIP4P	2.18	53.0	3.29
Exp.	2.95	78.4	2.30

Table 2: Computed values for the dipole moment, the dielectric constant, and self diffusion coefficient for SPC, TIP3P, and TIP4P models of water (see http://www.lsbu.ac.uk/water/models.html). Experimental values are given as a reference.

Exercise 3: Modeling Water. Using VMD and the saved state section05/models.vmd answer the following questions:
(1) What is the distance between the oxygen and hydrogen atoms?
(2) What is the angle formed by hydrogens and oxygen?
(3) By looking into the file section05/par_all27_prot_lipid.inp get the parameters utilized for the TIP3P water model. Be sure to include bond, angle, and Lennard-Jones terms. Hint: look for the words "TIP3P" or "TIPS3P".

5.2 Implicit Water Models

Usually, if not always, biomolecular systems need to be described in wet environments, where the role of the solvent may be essential. However, sim-

ulation of the solvent and the biomolecular system at the microscopic level can be prohibitive. We already described the parameterization difficulties of a molecular model of water. Furthermore, the cost of the computation of the interactions of all atoms is largely increased by the presence of an explicit solvent. Large reductions in computing time can be obtained if description of bulk solvent effects can be incorporated into the empirical potential function describing the biomolecular system through an implicit solvent model. This kind of implicit model needs to describe two important effects of a polar solvent: the solvation of charges embedded in a polar medium, and the damping of the electrostatic interaction between charges of the solute due to polarization by the medium. Most of the implicit models are based on the solution of the Poisson-Boltzmann equation or on the generalized Born approach. Other models include integral equations, stochastic methods, or screened Coulomb potentials (SCP) that allow calculation of electrostatic properties in proteins. Solvation energies and conduction properties of wide biological channels can be reasonably estimated using implicit solvent models over time scales that current simulations using explicit water models simply cannot reach. Although these implicit models permit the exploration of biomolecular systems over longer time scales, essential details may not be captured. For instance, hydrodinamical effects and the interaction of water with proteins forming and breaking water-protein hydrogen bonds during unfolding and folding is essential, and, thus, a description of the events at the atomic level is required.

6 Simulating Water

As one might be able to infer from Section 5, reproducing the macroscopic properties of water with either explicit or implicit models is not a simple task. In this section, we will test the TIP3P model of water with molecular dynamics simulations and analyze the results to give a feel for how these models are used in practice.

6.1 Simulation: Melting Ice

One of the most peculiar and challenging points of computational water modeling is the inability to reproduce freezing in simulated water molecules when the temperature is decreased below the experimental freezing point. Freezing of water in a simulation has been reported only one time in the

literature [21], however, multiple simulations on the order of microseconds were necessary to see a single freezing event. The work used the TIP4P model for water-water interaction.

In this section, we will not attempt to freeze liquid water, rather, we will try the opposite. Beginning with a lattice of ice, we will simulate the melting process.

We begin the simulation with the periodic ice lattice described in Section 2.2 and minimize the lattice for 1000 steps. The minimization simply allows the lattice to adjust slightly to accomodate inaccuracies in our force field, which was actually not parameterized for ice. After minimization, we begin a process of heating, starting at an initial temperature of 100 K and incrementing by 1 K every 2 ps. This heating protocol is somewhat unrealistic, since it corresponds to a temerature change of 500 billion K in one second. Ideally, the process should be much slower to allow equilibration after every temperature jump, but one is often constrained to short time simulations in molecular dynamics due to lack of computer power. Moreover, the heating protocol will still reveal interesting melting behavior.

We also run the simulation with periodic boundary conditions. Thus, we are effectively simulating an infinite ice lattice, so that water molecules on the edge will not cause premature melting. The initial boundary conditions must be chosen to take the exact dimensions of the ice lattice into account.

The results of the simulation reveal an interesting melting mechanism (see files section06/ICES.psf and section06/melting-sim/melt-100-grad2-01.dcd, or the movie melting.mpg). The ice lattice is preserved for the first 100 ps of simulation when the temperature reaches 150 K. At this point, a slight disruption in the lattice occurs and expands along a plane perpendicular to lattice vector 'b' until it stabilizes around 150 ps, when the temperature has reached 200 K. The simulation continues until the sheared melting region begins to expand when the simulation at 290 ps reaches 245 K. Melting occurs beginning with the shear plane and expanding rapidly over the next 20 ps (during which the temperature is raised by another 10 K) until the entire system is disordered and melted.

Two interesting issues arise from the results of the simulation. First, we must ask if the shearing which occurs is a natural phenomenon or if it is related to an inaccuracy of our forcefield. There is no definitive answer with the data available, however, one could run a second simulation whereby the water molecules have a different value for their angular spring constant. This might change the manner in which the shearing occurs or may prevent that

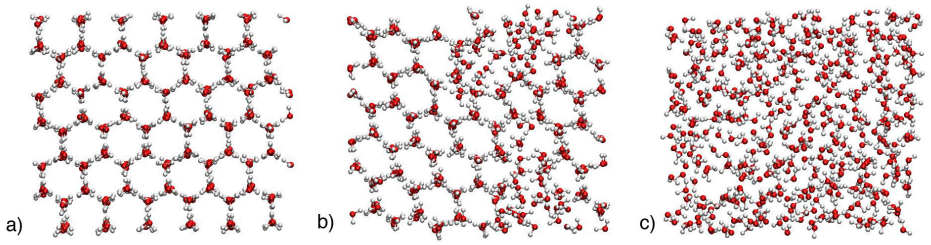

Figure 13: Ice melting simulation. Water molecule configurations are shown at three times and temperatures during the melting simulation: **a**) 20 ps, 110 K; **b**) 200 ps, 200 K; **c**) 400 ps, 300 K. Note the near perfect ice lattice at the beginning of the simulation which begins to melt due to lattice shearing. View the melting simulation with files section06/ICES.psf and section06/melting-sim/melt-100-grad2-01.dcd using VMD.

it occurs altogether.

The second issue which should be noticed is that the melting temperature is lower than the experimental value. This reflects the difficulty of reproducing macroscopic properties in the modeling of water. Water force field parameters are generally looking to reproduce quantities for liquid water at ambient room temperature since many of the chemical and biological processes to be studied occur at that condition. One might also argue, in fact, that obtaining a melting temperature which is 20-30 K different than experiment is quite good!

Exercise 4: Melting ice. The melting simulation is available in the directory section06/melting-sim/ as NAMD input and output files. Load the psf section06/ICES.psf and into it the dcd section06/melting-sim/melt-100-grad2-01.dcd in VMD and view the melting process.
Changing the angle spring constant of water may have an effect on the melting process shown. What changes in the process do you expect for a larger spring constant or for a smaller one?

6.2 Analysis: Pair Distribution Function*

In the previous simulation, we were able to observe the transition of ice to water. We knew definitively that the solid phase existed at the beginning of the simulation and that the liquid phase existed at the end. But what

happened during the melting process when it may have been unclear if a true liquid phase existed? Moreover, what about species different from water such as polymer gels, whose very nature make it difficult to distinguish a solid or liquid phase? Is there some way of quantifying the ordering to tell us which phase exists?

One way to observe the structural arrangement of molecules is through computing the pair distribution function. The pair distribution function $g(\mathbf{r}_i, \mathbf{r}_j)$, or $g(r)$ with $r = |\mathbf{r}_i - \mathbf{r}_j|$ for a homogeneous and isotropic material, is defined as "the probability of finding a pair of atoms at a distance r, relative to the probability expected for a completely random distribution at the same density" [22]. In the canonical ensemble the actual formula is

$$g(\mathbf{r}_1, \mathbf{r}_2) = \frac{N(N-1)}{\rho^2 \, Z_{NVT}} \int d\mathbf{r}_3 \, d\mathbf{r}_4 \ldots \exp(-\beta \mathcal{V}(\mathbf{r}_1, \mathbf{r}_2, \ldots \mathbf{r}_\mathbf{N})) \tag{3}$$

Here N is the total number of atoms, ρ is the density of the system, Z_{NVT} is the canonical partition function, $\beta = 1/kT$, and $\mathcal{V}$ is the potential energy governing the motion of the molecules. The pair distribution function can be obtained through a Fourier transformation of the structure factor obtained by x-ray and neutron diffraction patterns. Then, the experimentally determined values of the pair distribution function can be compared to the values computed using molecular models. An equivalent definition when using systems of identical atoms and useful for computer simulations is given by

$$g(r) = \frac{V}{N^2} \Big\langle \sum_i \sum_{j \neq i} \delta(\mathbf{r} - \mathbf{r}_{ij}) \Big\rangle \tag{4}$$

where $\langle \ldots \rangle$ denotes an ensemble average.

In order to gain a more intuitive knowledge of the pair distribution function, we analyze $g(r)$ computed for the oxygen atoms of liquid water as presented in Fig. 15. The value of $g(r)$ is 0 for $r \lesssim 2.5$ Å, meaning that the probability of finding two oxygen atoms at a distance $r \lesssim 2.5$ Å is zero. Does this make sense? Yes! Water molecules do not overlap, and hydrogen atoms share some room with oxygen atoms. Therefore, we should not find oxygen atoms too close to each other. The value of the pair distribution function suddenly increases for r increasing beyond 2.5 Å and reaches a maximum of ~ 3.8 at

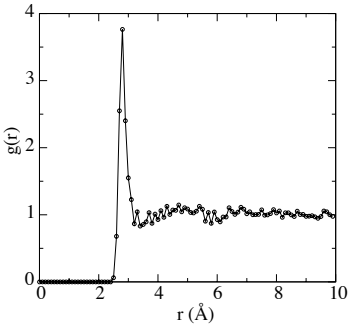

Figure 14: Pair distribution function for oxygens of liquid water (TIP3P model) computed us-

$r \sim 3$ Å. This maximum value of $g(r)$ means that if we pick a random oxygen atom in the system, and count the number of oxygen atoms surrounding it at a distance $r \sim 3$ Å, then we will find a number that is approximately three times larger than what we would have found in a completely random distribution of oxygen atoms at the same density. Is this reasonable? Yes! Hydrogen bonds between adjacent water molecules favor structured conformations of the molecules at short distances, even in liquid water. The value of the pair distribution function then decreases and fluctuates around one, reflecting the fact that at longer scales the structure of water molecules is lost, and the distribution of oxygen atoms is fairly random, as expected for liquid water. The pair distribution for oxygen atoms of water using the TIP3P water model described above compares reasonably well with experimental values. The theoretical model simulated seems to reproduce at least one of many properties of real water!

Exercise 5: Order in Water. Many structural properties can be tested using the pair distribution function. Using the provided scripts (section06/calcpdf.tcl and section06/pdf.tcl) along with VMD and the provided trajectories try to answer the following questions:
(1) How does the pair distribution function look like for liquid water when computed using hydrogen atoms only? Hint: Modify the script calcpdf.tcl in order to select hydrogens (name H1 H2) instead of oxygens (name OH2). The script is already set to use a trajectory of liquid water (melt-300-01.dcd). In order to use it, open the Tk Console in VMD and type "source calc.pdf" (make sure that you are in the right directory by using the commands "pwd" and "cd") and then plot the resulting list. How does the plot compares with Fig. 15?
(2) How does the pair distribution look like when computed on a crystal of water? Hint: Modify the script calcpdf.tcl so as to use the trajectory melt-10-01.dcd. Note that the computation of the pair distribution function is very demanding and it may take over 10 minutes to go over all the frames of the provided trajectories. While you wait, check the phases of water provided in the trajectories by opening another session of VMD, loading the file ICES.psf, and into it the trajectories melt-300-01.dcd and melt-10-01.dcd.

6.3 Theory: Temperature in Molecular Dynamics*

Determining the temperature of a substance is a simple task in practice, as long as one has a thermometer present. Complications may arise, however, when the amount of substance you want to measure is very small. For instance, determining the temperature of a microscopic object would be a considerable challenge. An ever greater challenge arises at the atomic level, when the very concept of temperature becomes skewed. Temperature is a macroscopic property. It is a single number that measures the average kinetic energy of a large system as a whole. How then are we to determine an accurate temperature for an atomic system, one in which the kinetic energy may vary wildly from atom to atom? Better yet, does temperature even have a meaning for very small systems like a single molecule of water? These questions need to be considered as one attempts an atomic representation of physical phenomena.

Molecular dynamics make use of the equipartition theorem of statistical mechanics [23] to determine the temperature of a simulation at any time. For a system of N atoms, the equipartition theorem equates the thermal energy of the system to the average kinetic energy of its atoms and accounts for any constraints on the atoms:

$$\frac{(3N - N_c)}{2} k_B T = E_{\text{kin}} \tag{5}$$

from which follows

$$T = \frac{2}{(3N - N_c)k_B} E_{\text{kin}} \ . \tag{6}$$

Here, N_c is the total number of internal constraints, such as fixed bonds, which may be the case for hydrogen atoms in a simulation, or fixed bond angles, which may be the case for some water models, as discussed earlier. Note that $3N - N_c$ is the total number of degrees of freedom of the system. Furthermore, note N_c also includes constraints that may be placed on the system to conserve momentum. In a system in which the momentum is fixed but no other constraints are placed on the atoms, $N_c = 3$, since the entire center of mass velocity is constrained to offset the atomic momenta.

With relationship (6), we can use the kinetic energy of the system as a "thermometer". The kinetic energy of a system of atoms at any time t is defined as

$$E_{\text{kin}}(t) = \frac{1}{2} \sum_{i=1}^{N} m_i |\mathbf{v_i}(t)|^2 \ . \tag{7}$$

In this equation the sum is over all atoms of the simulated sample. One can then express the instantaneous temperature of the system as

$$T(t) = \frac{1}{(3N - N_c)k_B} \sum_{i=1}^{N} m_i |\mathbf{v_i}(t)|^2 \; . \tag{8}$$

Furthermore, one can use the average kinetic energy of the system

$$\langle E_{\rm kin} \rangle = \left\langle \frac{1}{2} \sum_{i=1}^{N} m_i |\mathbf{v_i}|^2 \right\rangle \tag{9}$$

to define the average temperature of the system as

$$\langle T \rangle = \frac{2}{(3N - N_c)k_B} \left\langle \frac{1}{2} \sum_{i=1}^{N} m_i |\mathbf{v_i}|^2 \right\rangle \; . \tag{10}$$

In the above equations (9) and (10), the brackets denote a temporal average.

Figure 16 shows the time dependence of $T(t)$ for a simulated water system. One can recognize that $T(t)$ fluctuates around its average value $\langle T \rangle$. The right panel of Fig. 16 presents the sampled distribution of $T(t)$ values.

One can recognize from Fig. 16 that the temperature exhibits a Gaussian distribution around $\langle T \rangle$ with a width σ_T

$$p(T) \; = \; \frac{1}{\sqrt{2\pi\sigma_T^2}} \; \exp\left[-\frac{(T \; - \; \langle T \rangle)^2}{2\sigma_T^2} \right] \; . \tag{11}$$

Here, $p(T)$ is the probability of determining a system temperature T from the sample employing Eq. 8. The reason why the temperature readings produce a rather wide distribution is actually the finite size of the simulated system, as we will demonstrate below. In fact, the larger the system, the narrower the distribution of temperatures. This decrease in fluctuation with size may be understood if one thinks about a coin flip. On average, the probability of obtaining heads or tails is 50%. This is not the case, however, after you examine a single flip. The fluctuation from the average value is 50%! Upon increasing the number of flips, however, the deviation decreases as $1/\sqrt{N_{flips}}$.

In order to derive the distribution (11) from first principles, we begin with the fact that the velocity of each atom is distributed according to the well known Maxwell distribution. For each Cartesian component of the velocity,

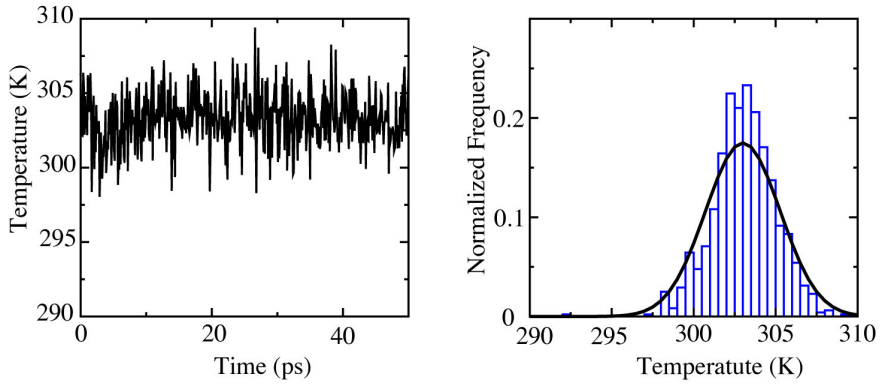

Figure 15: The left panel shows the instantaneous temperature computed for a periodic box of 11763 water molecules over a 50 ps molecular dynamics simulation. The right panel shows the corresponding distribution of temperatures sampled during the simulation (blue histogram) and the theoretically derived distribution (black).

e.g., for the x-component of the velocity of the jth atom, v_{jx}, the Maxwell distribution is

$$p(v_{jx}) \;=\; \sqrt{\frac{m_j}{2\pi k_B T}}\;\exp\left[-\frac{m_j}{2k_BT}\;v_{jx}^2\right] \tag{12}$$

and the average kinetic energy $\langle\epsilon_{jx}\rangle \;=\; \langle\frac{1}{2}m_j v_{jx}^2\rangle$ is accordingly

$$\langle\epsilon_{jx}\rangle \;=\; \sqrt{\frac{m_j}{2\pi k_B T}}\;\int_{-\infty}^{+\infty} dv_{jx}\,\frac{1}{2}m_j v_{jx}^2\;\exp\left[-\frac{m_j}{2k_BT}\;v_{jx}^2\right]\;. \tag{13}$$

Introducing the integration variable $y \;=\; \sqrt{m_j/2k_BT}\,v_{jx}$ leads to

$$\langle\epsilon_{jx}\rangle \;=\; \frac{k_BT}{\sqrt{\pi}}\;\int_{-\infty}^{+\infty} dy\;y^2\;\;\exp\left[-y^2\right]\;. \tag{14}$$

The integral arising here is equal to $\frac{1}{2}\sqrt{\pi}$. Hence, we find

$$\langle\epsilon_{jx}\rangle \;=\; \frac{1}{2}\;k_BT \tag{15}$$

which is the expected result. The average of the energy squared is

$$\langle\epsilon_{jx}^2\rangle \;=\; \sqrt{\frac{m_j}{2\pi k_B T}}\;\int_{-\infty}^{+\infty} dv_{jx}\,\left(\frac{1}{2}m_j v_{jx}^2\right)^2\;\exp\left[-\frac{m_j}{2k_BT}\;v_{jx}^2\right]\;. \tag{16}$$

Introducing the same integration variable y, we find

$$\langle \epsilon_{jx}^2 \rangle \;=\; \frac{(k_B T)^2}{\sqrt{\pi}} \int_{-\infty}^{+\infty} dy\; y^4 \;\; \exp\left[-y^2\right] \;. \tag{17}$$

The integral arising here is equal to $\frac{3}{4}\sqrt{\pi}$. Hence, we find

$$\langle \epsilon_{jx}^2 \rangle \;=\; \frac{3}{4}\,(\,k_B T\,)^2 \;. \tag{18}$$

The results described for $\langle \epsilon_{jx} \rangle$ and $\langle \epsilon_{jx}^2 \rangle$ permit us to determine the mean square deviation of the kinetic energy fluctuations. First, one derives the well known result

$$\langle\, (\epsilon_{jx}(t) - \langle \epsilon_{jx} \rangle\,)^2 \,\rangle \;=\; \langle\, (\,\epsilon_{jx}^2(t) - 2\,\epsilon_{jx}(t) \langle \epsilon_{jx} \rangle + \langle \epsilon_{jx} \rangle^2\,)\,\rangle \;=\; \langle \epsilon_{jx}^2 \rangle - \langle \epsilon_{jx} \rangle^2 \;. \tag{19}$$

Then, using Eqs. (15) and (18), we can conclude

$$\langle \epsilon_{jx}^2 \rangle \;-\; \langle \epsilon_{jx} \rangle^2 \;=\; \frac{1}{2}\,(k_B T)^2 \;. \tag{20}$$

From this follows the mean square fluctuation of the kinetic energy of the entire simulated system with $(3N \,-\, N_c)$ degrees of freedom

$$\sigma_E^2 \;=\; \langle E_{\rm kin}^2 \rangle \;-\; \langle E_{\rm kin} \rangle^2 \;=\; \frac{(3N \,-\, N_c)}{2}\,(k_B T)^2 \;. \tag{21}$$

One can define similarly the temperature fluctuation σ_T, and using the definition of T as given in Eqs. (9) and (10), one concludes

$$\sigma_T^2 \;=\; \langle T^2 \rangle \;-\; \langle T \rangle^2 \;=\; \frac{4}{(3N \,-\, N_c)^2\, k_B^2}\;\sigma_E^2 \tag{22}$$

or

$$\sigma_T^2 \;=\; \frac{2T^2}{3N \,-\, N_c} \;. \tag{23}$$

From our derivation we conclude that over the course of a simulation, the temperature will change even when the system is in equilibrium. Deviations in atomic interactions will cause changes in atomic velocities, so an equilibrated system whose temperature is 300 K at one time may later have a temperature of 297 K at another time and a temperature of 305 K still later. The above result states that the temperature distribution shown in Fig. 16

should be characterized through a width that depends on temperature and particle number. As one can see in Fig. 16, the Gaussian distribution with a width predicted by Eq. (23) matches the simulated distribution. One concludes therefore that the observed temperature fluctuation in the simulation is a finite size effect, with relative fluctuations on the order of $1/\sqrt{3N - N_c}$.

References

[1] D. Voet, J. G. Voet, and C. W. Pratt. *Fundamentals of Biochemistry.* John Wiley & Sons, Inc., New York, 1999.

[2] D. R. Lide, editor. *CRC Handbook of Chemistry and Physics.* CRC Press, Boca Raton, 74th edition, 1994.

[3] P. L. Davies, J. Baardsnes, M. J. Kuiper, and V. K. Walker. Structure and function of antifreeze proteins. *Phil. Trans. R. Soc. Lond. B*, 357:927–935, 2002.

[4] C. A. Knight, C. C. Cheng, and A. L. DeVries. Adsorption of alpha-helical antifreeze peptides on specific ice crystal surface planes. *Biophysical Journal*, 59:409–418, 1991.

[5] J. D. Madura, K. Baran, and A. Wierzbicki. Molecular recognition and binding of thermal hysteresis proteins to ice. *Journal of Molecular Recognition*, 13:101–113, 2000.

[6] S. M. McDonald, A. White, P. Clancy, and J. W. Brady. Binding of an antifreeze polypeptide to an ice/water interface via computer simulation. *AIChe*, 41(4):959–973, 1995.

[7] Z. Jia, C. I. DeLuca, H. Chao, and P. L. Davies. Structural basis for the binding of a globular antifreeze protein to ice. *Nature*, 384:285–288, 1996.

[8] A. L. DeVries. Antifreeze proteins and glycopeptides in cold-water fishes. *A. Rev. Physiol.*, 45:245–260, 1983.

[9] A. W. Adamson. *Physical Chemistry of Surfaces.* John Wiley & Sons, 3rd edition, 1976.

[10] P. Atkins and J. de Paula. *Atkins' Physical Chemistry*. Oxford University Press, 2002.

[11] F. Heslot, N. Fraysse, and M. Cazabat. Molecular layering in the spreading of wetting liquid drops. *Nature*, 338:640–642, 1989.

[12] P. Roura and J. Fort. Local thermodynamic derivaiton of young's equation. *Journal of Colloid and Interface Science*, 272:420–429, 2004.

[13] R. Lamb and N. Furlong. Controlled wettability of quartz surfaces. *Journal of the Chemical Society-Faraday Transactions*, 78:61–73, 1982.

[14] A. Bródka and T. W. Zerda. Properties of liquid acetone in silica pores: Molecular dynamics simulation. *Journal of Chemical Physics*, 104:6319–6326, 1996.

[15] J. Hill and J. Sauer. Molecular mechanics potential for silica and zeolite catalysts based on ab initio calculations. 1. dense and microporous silica. *Nature*, 338:640–642, 1989.

[16] X. Gao and L. Jiang. Water-repellent legs of water striders. *Nature*, 432:36, 2004.

[17] D. L. Hu, B. Chan, and J. W. M. Bush. The hydrodynamics of water strider locomotion. *Nature*, 424:663–666, 2003.

[18] L. Feng, S. Li, Y. Li, H. Li, L. Zhang, J. Zhai, Y. Song, B. Liu, L. Jiang, and D. Zhu. Super-hydrophobic surfaces: From natural to artificial. *Advanced Materials*, 14:1857–1860, 2002.

[19] J. L. Finney. The water molecule and its interactions: the interaction between theory, modelling, and experiment. *Journal of Molecular Liquids*, 90:303–312, 2001.

[20] W. L. Jorgensen, J. Chandrasekhar, J. D. Madura, R. W. Impey, and M. L. Klein. Comparison of simple potential functions for simulating liquid water. *JCP*, 79:926–935, 1983.

[21] M. Matsumoto, S. Saito, and I. Ohmine. Molecular dynamics simulation of the ice nucleation and growth process leading to water freezing. *Nature*, 416:409–413, 2002.

[22] M. P. Allen and D. J. Tildesley. *Computer Simulation of Liquids*. Oxford University Press, New York, 1987.

[23] Kerson Huang. *Statistical Mechanics*. Wiley Eastern Limited, New Delhi, 1988.